ELSEVIER

Investigating ponding depth and soil detachability for a mechanistic erosion model using a simple experiment

Bin Gao[a], M.T. Walter[a,*], T.S. Steenhuis[a], J.-Y. Parlange[a], K. Nakano[a], C.W. Rose[b], W.L. Hogarth[c]

[a]Department of Biological and Environmental Engineering, Cornell University, Ithaca, NY 14853-5701, USA
[b]Faculty of Environmental Sciences, Griffith University, Nathan, Qld 4111, Australia
[c]Faculty of Science and Information Technology, University of Newcastle, Callaghan, NSW 2308, Australia

Abstract

This work extends the simple experimental studies initiated by Heilig et al. [J. Hydrol. 244(2001) 9] to study erosion processes inherent to a mechanistic soil erosion model (the Rose model) that were not addressed in earlier studies. Specifically, we investigated the impacts of ponding water depth and soil detachability on erosion. The Rose model describes the interplay among the processes of soil detachment, transport, deposition, and redetachment, which are involved in rain-induced soil erosion and sediment transport. The simple experiment that was used to improve our understanding of how water-ponding and soil detachability affect soil erosion utilized a small, horizontal, uniform, soil surface exposed to uniform, simulated rainfall. Rainfall rates were systematically changed between 6 and 48 mm h^{-1}. Soil detachability was associated with a clay soil prepared at two different water contents. The Rose model was applied to the experimental conditions and the predicted erosion behavior was compared to experimental measurements. Observed data compared very well with the model results. The experimentally observed relationship between ponding water depth and soil detachability agreed well with previously proposed theories; soil detachability was constant for ponding depths below a critical depth and dramatically decreased above the critical depth. Also, these experiments corroborated that the soil detachability as represented in the Rose model is independent of rain intensity. These results provide support to the validity of the Rose model with respect to the roles of surface water-ponding and its relationship to soil detachability. These mechanisms can be incorporated into models of more complicated and realistic systems in which these individual processes may be difficult to explicitly identify.
© 2003 Elsevier Science B.V. All rights reserved.

Keywords: Soil erosion; Mechanistic model; Surface water ponding; Soil detachability; Raindrop detachment

1. Introduction

[Rose and Dalal, 1988, Hairsine and Rose (1991) and Rose et al. (1994,1998)](#) developed a physically

* Corresponding author. Tel.: +1-607-255-2488; fax: +1-607-255-4080.
  E-mail address: mtw5@cornell.edu (M.T. Walter).

based model of rain impact soil erosion, which considers soil erosion from raindrop impact and sediment transport in overland flow. In its simplest form, the model assumes that shear forces from runoff are negligible relative to rain impact forces for interrill soil erosion. The Rose model provides a basis for understanding the interaction of rainfall detachment and deposition of cohesive soils

composed of a range of particle and aggregate sizes and densities (Sander et al., 1996):

$$\frac{\partial(c_i q)}{\partial x} + \frac{\partial(c_i D)}{\partial t} = e_i + e_{di} - d_i \qquad (1)$$

where c_i is the concentration of soil particles (size class i) in the surface flow [ML^{-1}], D is the flow depth [L], and q is the volumetric overland flow [L^2T^{-1}]. The terms e_i and e_{di} are the rates of soil detachment from the original soil and redetachment from deposited soil of class-i particles. The term d_i is the rate of deposition of class-i particles. The Rose model's conciseness makes it look deceptively simple, but it incorporates multiple, interdependent erosional processes such as particle detachment, deposition, and redetachment (Fig. 1). The Rose model has been fully described in many previous articles (Hairsine and Rose 1991; Rose et al., 1994; Sander et al., 1996; Lisle et al., 1998; Parlange et al., 1999).

Proffitt et al. (1991) performed a set of laboratory experiments that demonstrated the model's ability to predict sediment delivery at the bottom of a hillslope. As pointed-out by Heilig et al. (2001), although Proffitt et al. (1991) experiments have corroborated Rose model predictions (Sander et al., 1996; Parlange et al., 1999), the experiments were designed to replicate natural erosion and, as a result, they were too complicated to directly elucidate the individual,

Fig. 1. Schematic of the Rose model's fundamental processes.

fundamental erosion processes. In response, Heilig et al. (2001) successfully used a simple experiment to visually and analytically verify the conceptual basis of the Rose model with special attention to the development of a surface shield composed of deposited heavy soil particles; this shielding process is unique to the Rose model. To isolate the shielding process, it was necessary for Heilig et al. (2001) to create a simple, small scale experiment that eliminated as many extraneous processes as possible, one of which was dynamic ponding depth over the soil. The use of a steady-state ponding depth simplified the analytical modeling but also introduced some experimental difficulties. Specifically, it was difficult to design a container that simultaneously maintained a constant ponding depth and did not let any shield-particles escape. Heilig et al. (2001) noted some systematic, although small, discrepancies that may have been attributable to these experimental problems.

This study is an extension of the on-going investigation initiated by Heilig et al. (2001) to use simple bench-scale experiments to elucidate individual erosion processes that are incorporated in the Rose model. Specifically, this paper focuses on the role of water-ponding dynamics on soil erosion by using an experimental apparatus similar in scale to Heilig et al. (2001) that avoids the experimental problems noted above by not letting any water or soil escape. This experiment allows us to investigate how water-ponding and soil detachment affect soil erosion and the behavior of the associated parameters in the Rose model. Whereas Heilig et al. (2001) experimental design facilitated eliminating the $\partial(c_i D)/\partial t$ term from Eq. (1); the experiment used in this study eliminates the $\partial(c_i q)/\partial x$ term. Specifically investigated were the relationships among soil detachment, ponding water depth, and rainfall intensity and the reasonableness of previously proposed expressions involving these parameters. To simplify the experimental design and mathematical investigation, this study does not consider the shielding processes previously studied by Heilig et al. (2001).
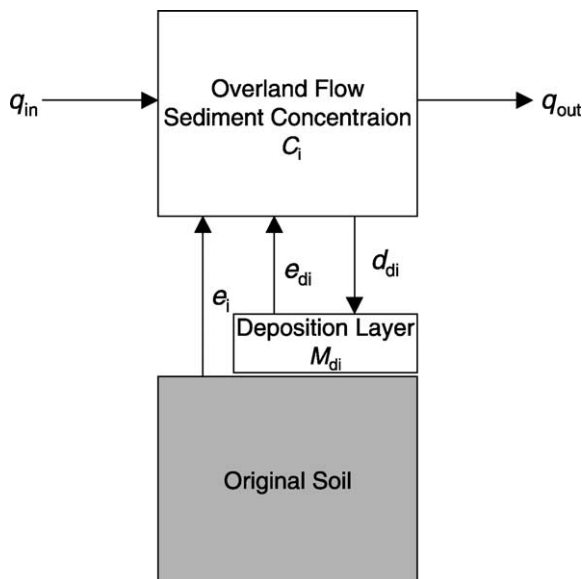
2. Experimental design

The experimental set-up is simple and designed to isolate the roles of soil detachment and water-ponding

in soil erosion. A small, cylindrical, Plexiglas container (column with cross-sectional area, $A = 45$ cm^2) was filled with man-made soil and leveled 3 m below a computer- controlled rainmaker (Fig. 2). After carefully establishing a flat soil surface, rain was simulated over the container. Two sets of six different experiments were run at different rain intensities (6–48 mm h^{-1}); each set utilized one of two kinds of artificial soils. The container has no outlets so the ponding depth was simply equal to the precipitation rate multiplied by elapsed time. The ponded water was periodically sampled from the middle of the water column using a 0.05 ml pipette. The first sample was taken when the ponding depth was approximately 2 mm and subsequent sampling occurred every 1–5 min depending on the rainfall rate. Later, samples were collected at longer intervals as the dynamic behavior of the system slowed. Each experiment continued until the ponded water was about 25 mm. The sediment concentration of each sample was measured using the same spectrophotometer and methods used by Heilig et al. (2001).

Two types of man-made, uniform soil were considered in order to investigate different soil detachabilities. Both soils consisted of clay particles (hydrous Kaolin supplied by Englehard Corp, NJ) alone. Clay settles-out of water very slowly, i.e. settling velocity ≈ 0, deposition and redetachment processes play negligible roles in these experiments. Also, unlike Heilig et al. (2001), no surface shield can develop. Thus, this choice of soil particle provided opportunities to simplify the model by eliminating unnecessary processes. Each of the two soils had a unique water content, one was 'saturated' (by mass, 4 parts water: 5 parts clay) and the other unsaturated (by mass, 3 parts water: 4 parts clay). We refer to the wetter soil as 'saturated' because mixing any additional water led to surface ponding. The soil was put into a 3 cm high Plexiglas container and the surface was smoothed. Then a 15 cm high column was glued on the container to keep the ponding water from leaving the system (Fig. 2). The experiment was covered until constant rainfall was established, after which a timer was started and the cap was removed simultaneously.

Improving on Heilig et al. (2001) rainfall simulations, a computer-controlled rainmaker that oscillated simultaneously along two orthogonal tracks
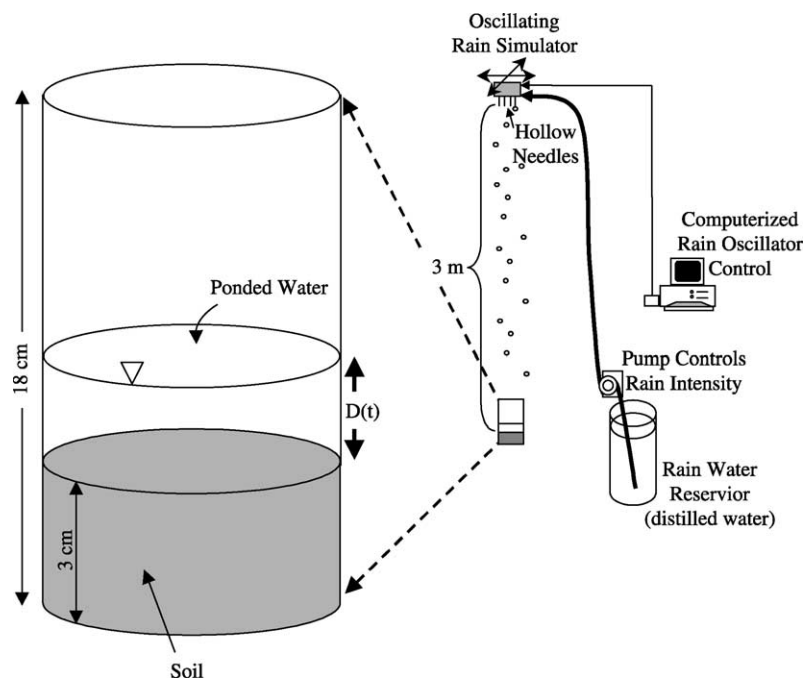

Fig. 2. Schematic of the experimental apparatus and set-up.

was used to better control the spatial uniformity and randomness of rainfall. Identical hypodermic needles were used to maintain uniform and constant raindrop sizes (~ 0.05 ml), so that experimental results could be related rainfall intensity, which is easily measured directly, rather than the kinetic energy of the rain. The rainmaker was attached to the ceiling of the soil and water laboratory at Cornell University's Biological and Environmental Engineering Department, 3 m above the soil surface. Rainfall intensity was controlled with a variable speed pump that supplied water to the rainmaker. Uniformity was measured identically to Heilig et al. (2001). The simulated rainfall consistently had uniformity of >0.9, and the rain intensity was tested twice before and once after each experiment.

3. Results and discussion

The model can be substantially simplified if it is applied to our simple experiment. Specifically, our experiment uses only one particle class, assumes no deposition because we use small clay particles that remain suspended, and has no overland flow. For this situation, (1) can be expressed as:

$$\frac{\mathrm{d}(cD)}{\mathrm{d}t} = e \tag{2a}$$

or:

$$\frac{\mathrm{d}M}{\mathrm{d}t} = e \tag{2b}$$

where M is the total mass per area of sediment in the ponded-water and under the complete mixing assumption, $M = cD$. The soil detachability is a ubiquitous term used to describe a soil's susceptibility to erosion. Rose et al. (1994) and others have proposed the following function relating rainfall-induced soil detachment per unit area of soil, e, to soil detachability and rainfall intensity, P:

$$e = aP^p \tag{3}$$

where P is the rainfall rate $[LT^{-1}]$, the parameter a is the bare soil's detachability, and p is a constant. The constant exponent, p, is usually assumed to be unity although it has received very little experimental study, until now. Note that Eq. (3) differs slightly from
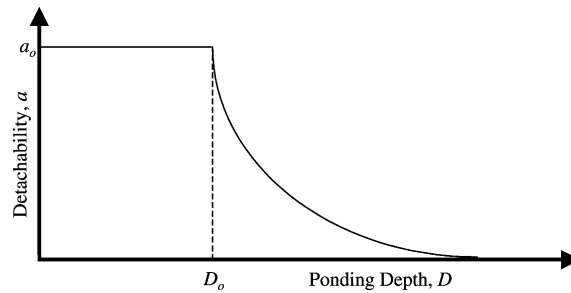

Fig. 3. Theoretical relationship between soil detachment, a and pond-depth, D. D_0 is the critical depth separating the shallow-ponded erosion regime from the deep-ponded regime.

analogous expressions used in previous studies, which typically accounts for surface shielding with an additional multiplier in Eq. (3) (e.g. Proffitt et al., 1991; Heilig et al., 2001). Because our experiment was designed to eliminate the complexities of surface shielding we have simplified Eq. (3) accordingly. Several researchers have suggested that the soil detachability is constant when the ponding depth or flow depth, D, is below a critical or breakpoint depth, D_0, and that soil detachability is reduced for $D > D_0$ (Fig. 3) (Moss and Green, 1983; Proffitt et al., 1991; Hairsine and Rose, 1991):

$$a = a_0 \text{ for } D \le D_0 \tag{4a}$$

$$a = a_0(D_0/D)^b \qquad \text{for } D > D_0 \tag{4b}$$

where b is a positive constant and, for these experiments, $D = Pt$.

Fig. 4 shows the data for all the experiments plotted with respect to ponding depth; plotted in this form the experimental data from the different rain intensities should, if $p = 1$, hypothetically superimpose themselves on top of each other for each soil type. Despite the scatter in the data, both soils exhibit two identifiable erosion regimes (Fig. 4). The early, or shallow-ponded, regime is characterized by a linearly increasing mass of eroded material in suspension. The late, or deep-ponded, regime is generally flat, i.e. no additional material went into suspension during this period. For the shallow-ponded regime the data nearly lie on top of each other as expected. Unlike the shallow-ponded regime, however, the deep-ponded regime shows substantial scatter in the data but the lack of an obvious systematic trend suggests that this scatter is random and inherent in the experimental
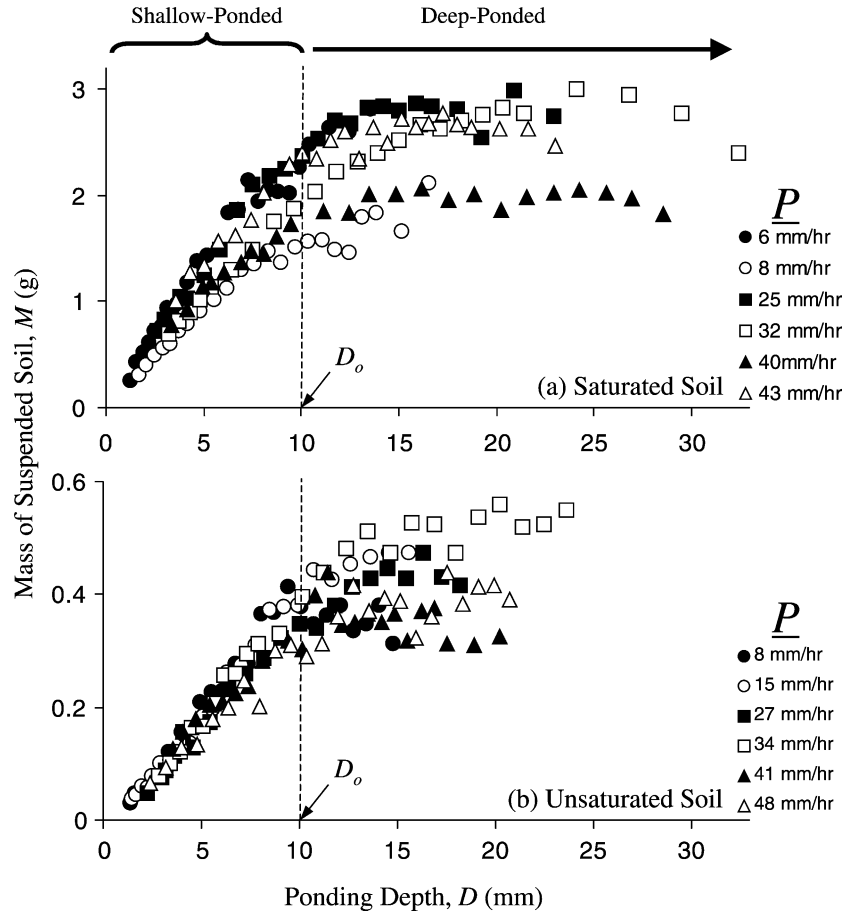
Fig. 4. Experimental results for the saturated (a) and unsaturated (b) soils. Each symbol is a unique experimental run with unique rainfall intensity, P, as indicated in each figure. The dashed line shows the approximate critical depth separating the shallow-ponded erosion regime from the deep-ponded.

design. Because of the scatter, it is not possible to precisely identify a critical ponding depth, D_0, in Fig. 4 but the transition between erosion regimes is roughly at a depth of ~ 10 mm for both soils. The critical depth is the depth at which the ponded water absorbs enough of the raindrop energy and, because the raindrop characteristics were the same for all experiments, the raindrop's energy should have been similar for all experiments independent of soil type or rain intensity. Thus, the observed similarity in D_0 between the two soil types is expected. Note that soil particle size probably influences D_0 and both soils were composed of the same size particles.

We used $D_0 = 10$ mm as an approximate value for the critical depth in order to investigate the soil

detachability, a_0, and exponential constant, p, for the shallow-ponded, $D < D_0$, or early, $t < t_0$, erosion regimes, where t_0 is the time at which $D = D_0$. The critical time, t_0, was calculated for each experiment and the data were plotted against time as shown in Fig. 5. For each experiment a linear regression was performed on the data for $t < t_0$ (Fig. 5) and the slope of the regression line is dM/dt, which is the erosion rate, e, as shown in Eq. (2b). Table 1 shows the erosion rates, e, and the regression R^2s for all the experiments. The correlation between the total mass of clay in the ponded water, M, and time, t, was good for all the experiments, $R^2 > \sim 0.9$. Note that all regressions were assumed to intercept the origin.
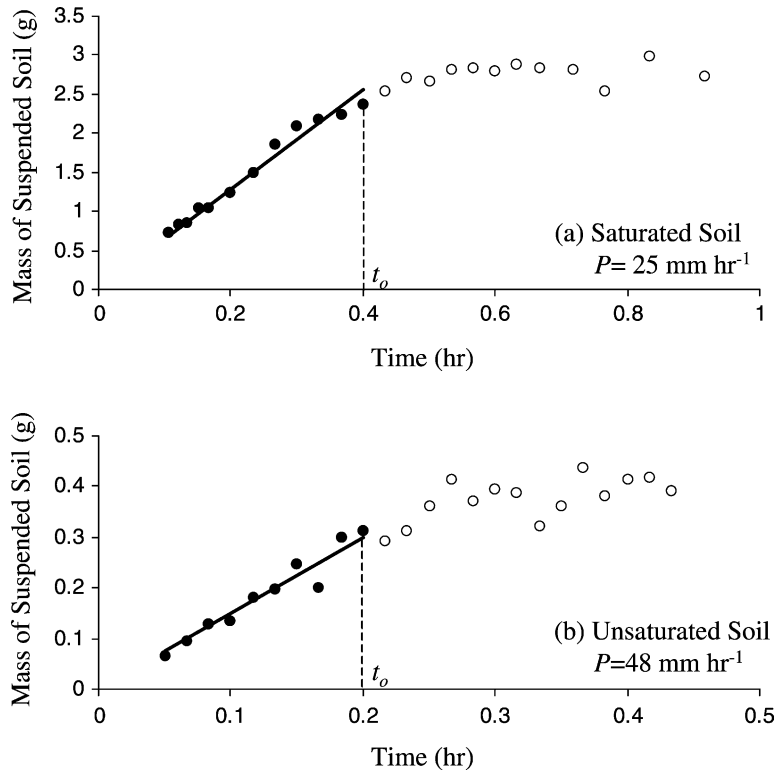
Fig. 5. Example mass–time curves for the saturated (a) and unsaturated (b) soils. The dark symbols show data during the early part of the experiment, $t < t_0$, and the light symbols show data for the late part of the experiment. The lines are the linear regressions for the early, or shallow-ponded, erosion regimes. Table 1 shows results for all experiments.

Fig. 6 shows the relationship between e and P for all the experiments and suggests that the constant $p = 1$ ($R^2 > 0.9$). This supports the assumption of unity assumed by several researchers (Sander et al., 1996; Heilig et al., 2001) and corroborates results by Sharma et al. (1993, 1995) and Jayawardena and Bhuiyan (1999). Interestingly, several earlier studies suggested

$p = 2$ (Meyer, 1982; Foster, 1982; Liebenow et al., 1990), which was originally used in the USDA WEPP model (Laflen et al., 1991).

The slopes of the relationships in Fig. 6 are unique to each soil type and represent the soil detachability, a_0. The saturated soil has a much higher detachability, a_0, than the unsaturated; the saturated soil detach-

Table 1
Rainfall rates and regression results for M vs. t as shown in Fig. 5

	Saturated soil			Unsaturated soil		
	P (mm h^{-1})	e^a (g h^{-1})	R^2	P (mm h^{-1})	e^a (g h^{-1})	R^2
Run1	6	1.73	0.98	8	0.32	0.96
Run2	8	1.52	0.99	15	0.54	0.96
Run3	25	6.20	0.97	27	0.94	0.97
Run4	32	6.41	0.98	34	1.28	0.97
Run5	40	7.91	0.84	41	1.36	0.92
Run6	43	10.77	0.95	48	1.50	0.94

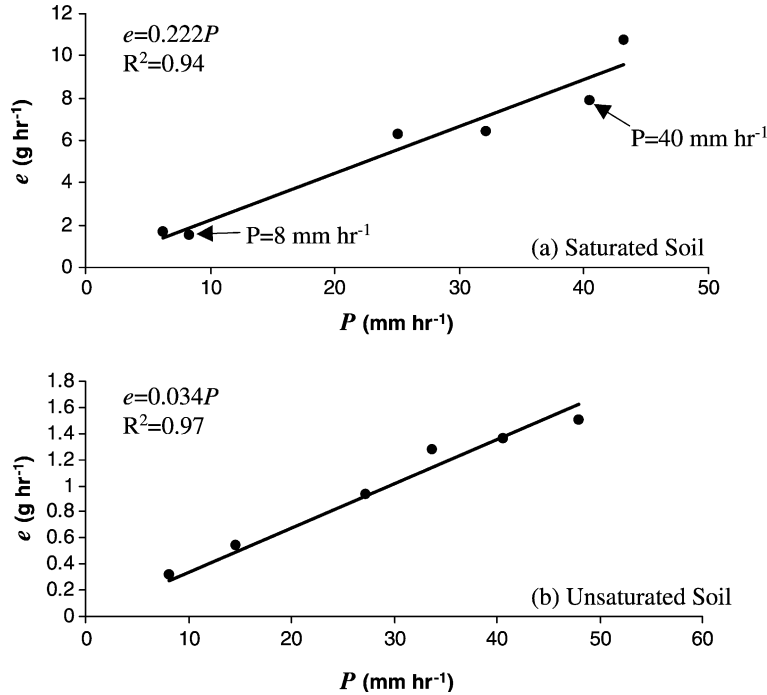[a] e, the erosion rate, is the slope of the M vs. t regression (e.g. Fig. 5).

Fig. 6. Erosion rate, e, vs. rainfall rate, P, for the saturated soil (a) and unsaturated (b) soils. Symbols represent data from Table 1 and the lines are the linear regressions.

ability ~ 0.22 g mm^{-1} and the unsaturated soil detachability ~ 0.034 g mm^{-1}. This is expected because saturated soil had less cohesion between particles than drier soil. The points corresponding to $P = 8$ mm h^{-1} and $P = 40$ mm h^{-1} are indicated in Fig. 6a. These points correspond to the experimental runs that may appear to be outliers in Fig. 4 (the open circles and solid triangles) and are specifically indicated to show that their apparent disagreement with the other runs does not seem to affect their contribution in this analysis. In fact, removing either or both of these points had no impact on the calculated detachability at our reported precision.

The next step in this study was to check how well the Rose model fit the data for all times, an exercise that facilitates more precise estimates for the critical depth, D_0 and additional estimates of a_0. To do this, we solved the Rose model, as expressed in Eqs. (2a) and (2b), using our experimentally determined estimate for p (i.e. $p = 1$), and the theoretical $a(D)$ relationship, Eq. (4a) and (4b), to get the following:

$$M = a_0Pt \qquad \text{for } t \leq t_0 \tag{5a}$$

$$M = M_0 + \frac{a_0Pt_0^b(t^{1-b} - t_0^{1-b})}{1 - b} \tag{5b}$$

for $t > t_0$ $(b \neq 1)$

$$M = M_0 + a_0Pt_0 \ln\left(\frac{t}{t_0}\right) \qquad \text{for } t > t_0 \ (b = 1) \tag{5c}$$

where $M_0 = a_0Pt_0$ and t_0 is the time when $D = D_0$. The parameter b, from Eqs. (4a) and (4b) is still unknown. Recalling that the experimental design dictates $D(t) = Pt$, Eqs. (5a)–(5c) can be written in terms of depth:

$$M = a_0D \qquad \text{for } D \leq D_0 \tag{6a}$$

$$M = M_0 + \frac{a_0D_0^b(D^{(1-b)} - D_0^{(1-b)})}{1 - b} \tag{6b}$$

for $D > D_0$, $\qquad$ (if $b \neq 1$)

$$M = M_0 + a_0D_0 \ln\left(\frac{D}{D_0}\right) \tag{6c}$$

for $D > D_0$ (if $b = 1$)

Fig. 7 shows the modeled (Eqs. (6a)–(6c)) and average measured suspended mass, M, vs. ponding depth, D, for all the experiments using a best fit b and $b = \infty$ to describe the late, deep-ponded, erosion regime, i.e. for $D > D_0$. The error bars in Fig. 7 show the entire span of observed data used to calculate each average data point. For each value of b, the model was best-fit to the data by changing D_0 and a_0. Because of the high degree of freedom in fitting the model to the data a unique, best-fit b was difficult to identify, however $b > 3$ resulted in $R^2 > 0.98$ for both soils. Interestingly, $D_0 s$ determined using the Rose model are within ~ 1.5 mm of our original estimate, $D_0 = 10$ mm, which we assumed was imprecise.
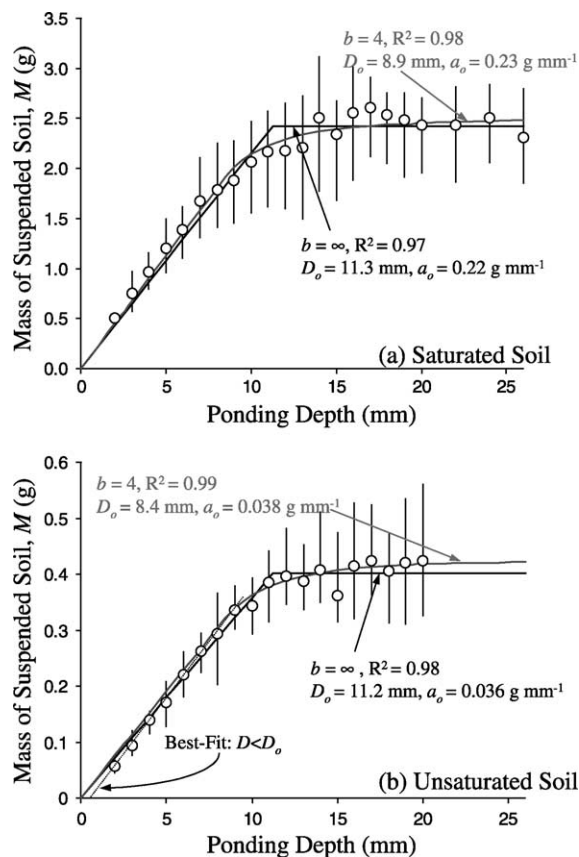

Fig. 7. Model and experimental results for the saturated (a) and unsaturated (b) soils. Symbols are averages from all experiments, error bars indicated the entire range of observed values, and solid lines are the model results: red and black lines correspond to b values (Eq. (6)) of 4 and ∞, respectively. Critical depths, D_0, soil detachabilities, a_0, and R^2 for each model are shown on the graphs.

The soil detachability, a_0, determined by fitting the Rose model (Eqs. (6a)–(6c)) was similar or slightly higher than the earlier experimental results, differences ≤ 0.01 g mm^{-1}.

It is also interesting that the simplest relationship for soil detachability, a, as a function of ponding depth D, namely the step function, $b = \infty$, works almost as well as the finite b (Fig. 7). This is especially true of the unsaturated soil (Fig. 7). Because of saturated soil's high susceptibility to erosion, i.e. its high soil detachability, it is likely that rain-impact energy transferred through the ponded water via eddies would continue to have a more pronounced impact on saturated soil than on the unsaturated soil at ponding depths above D_0. This may explain why, in Fig. 7, the unsaturated soil transition appears more sharply than the saturated soil between the shallow-ponded and deep-ponded erosion regimes. The step function for $a(D)$, of course, fits a sharp transition best.

Notice that the best-fit time for the early, or shallow-ponded, erosion period in Fig. 7b deviates slightly from the model and crosses the 'ponding depth' axis around 1 mm. Although this deviation was too small to seriously affect the results of this study, which used generally wet soils, it supports the anticipated future direction of our investigations, namely how infiltration affects rain-impact erosion and how the Rose model represents these processes.

As a final note, it appears in Fig. 4 that for long times, i.e. deep ponding depths, that the suspended mass may be beginning to decrease for some experiments suggesting the settling velocity was not zero but it is so small that settling can, indeed, be ignored for short times. The possible indications of settling activity in Fig. 4 are only apparent long after D_0 was achieved and, therefore, the assumption of negligible settling does not impact our conclusions. Although there may be settling during the initial phases of this experiment, it is likely that raindrop impact in shallow water will provide enough turbulence to keep clay suspended. Some of the scatter in the data for the deep-ponded period may have arisen due to stratification of sediment-solutions from which well-integrated sampling was difficult, i.e. the complete mixing assumption may have been violated when the ponding water was deep.

4. Conclusion

The ponding-water depth and soil detachment aspects of the Rose soil erosion model were illustrated and tested using a very simple experiment. The experimental data agreed well with the model results and two important model constants were parameterized, the soil detachability, a_0, and the critical ponding depth, D_0. Our study showed that when the ponding depth is less than D_0, the soil detachability due to raindrop impact is constant for a given soil type and moisture content. In these experiments, the soil detachability, a, rapidly decreased with the growth of the ponding water depth, D, above D_0. This is perhaps our most important result because if $a(D)$ can be assumed to be a step function, it eliminates an otherwise unknown parameter, i.e. b, from the model and simplifies analytical approaches to the Rose model. These experiments also corroborated previous studies by Heilig et al. (2001), that the value of the exponent p in the detachment Eq. (3) is unity or very nearly so. The suite of simple studies, of which this is one, provides insights into soil erosion and the Rose model and suggests methods for parameterizing similar mechanistic soil erosion models.

References

Foster, G.R., 1982. Modeling the erosion process. In: Haan, C.T., (Ed.), Hydrological Modeling of Small Watersheds, Monograph No. 5, ASAE, St Joseph, MI, pp. 297–379.

Hairsine, P.B., Rose, C.W., 1991. Rainfall detachment and deposition: sediment transport in the absence of flow-driven processes. Soil Sci. Soc. Am. J. 55 (2), 320–324.

Heilig, A., DeBruyn, D., Walter, M.T., Rose, C.W., Parlange, J.-Y., Sander, G.C., Hairsine, P.B., Hogarth, W.L., Walker, L.P., Steenhuis, T.S., 2001. Testing of a mechanistic soil erosion model with a simple experiment. J. Hydrol. 244 (1–2), 9–16.

Jayawardena, A.W., Bhuiyan, R.R., 1999. Evaluation of an interrill soil erosion model using laboratory catchment data. Hydrol. Proc. 13, 89–100.

Laflen, J.M., Elliot, W.J., Simanton, J.R., Holzhey, C.S., Khol, K.D., 1991. WEPP soil erodibility experiments for rangeland and cropland soils. J. Soil Water Conserv. 49 (1), 39–44.

Liebenow, A.M., Elliot, W.J., Laflen, J.M., Kohl, K.D., 1990. Interrill erodibility-collection and analysis of data from cropland soils. ASAE Trans. 33 (6), 1882–1888.

Lisle, I., Rose, C.W., Hogarth, W., Hairsine, P., Sander, G., Parlange, J.-Y., 1998. Stochastic sediment transport in soil erosion. J. Hydrol. 204 (1–4), 217–230.

Meyer, L.D., 1982. Soil-erosion research leading to development of the universal soil erosion loss equation. Sci. Education Adm. Pub. ARM NW-26, 1–16.

Moss, A.J., Green, P., 1983. Movement of solids in air and water by raindrop impact—effects of drop-size and water-depth variations. Aust. J. Soil Res. 21 (3), 257–269.

Parlange, J.-Y., Hogarth, W.L., Rose, C.W., Sander, G.C., Hairsine, P., Lisle, I., 1999. Note on analytical approximations for soil erosion due to rainfall impact and for sediment transport with no inflow. J. Hydrol. 217, 149–156.

Proffitt, A.P.B., Rose, C.W., Hairsine, P.B., 1991. Rainfall detachment and deposition: experiments with low slopes and significant water depths. Soil Sci. Soc. Am. J. 55, 325–332.

Rose, C.W., Dalal, R.C., 1988. Erosion and runoff of nitrogen. In: Wilson, J.R., (Ed.), Advances in Nitrogen Cycling in Agricultural Ecosystems, CAB International, Wallingford, England, pp. 212–235.

Rose, C.W., Hogarth, W.L., Sander, G., Lisle, I., Hairsine, P., Parlange, J.-Y., 1994. Modeling processes of soil erosion by water. Trends Hydrol. 1, 443–451.

Rose, C.W., Parlange, J.-Y., Lisle, I.G., Hogarth, W.L., Hairsine, P.B., Sander, G.C., 1998. Unsteady soil erosion due to rainfall impact and sediment transport. In: Morel-Seytoux, H., (Ed.), Hydrology Days, vol. 18. AGU Pub, pp. 245–258.

Sander, G.C., Hairsine, P.B., Rose, C.W., Cassidy, D., Parlange, J.-Y., Hogarth, W.L., Lisle, I.G., 1996. Unsteady soil erosion model, analytical solutions and comparison with experimental results. J. Hydrol. 178, 351–367.

Sharma, P.P., Gupta, S.C., Foster, G.R., 1993. Predicting soil detachment by raindrops. Soil Sci. Soc. Am. J. 57, 674–680.

Sharma, P.P., Gupta, S.C., Foster, G.R., 1995. Raindrop-induced soil detachment and sediment transport from interrill areas. Soil Sci. Soc. Am. J. 59, 727–734.